Dissipative and conservative nonlinearity in carbon nanotube and graphene mechanical resonators

J. Moser,[1] A. Eichler,[1] B. Lassagne,[1] J. Chaste,[1] Y. Tarakanov,[2] J. Kinaret,[2] I. Wilson-Rae,[3] and A. Bachtold[1]

[1]*Institut Catalá de Nanotecnologia, Bellaterra 08193, Spain*

[2]*Department of Applied Physics, Chalmers University of Technology, Göteborg 41296, Sweden*

[3]*Technische Universität München, Garching 85748, Germany*

PACS numbers:

I. INTRODUCTION

Graphene and carbon nanotubes are excellent materials for nanoelectromechanical systems (NEMS). Their large stiffness and low density allow to fabricate high frequency mechanical resonators sensitive to minute variations of mass, force, and charge[1–25]. In addition to their outstanding mechanical properties, these materials owe part of their uniqueness to their simplest feature: They constitute the ultimate size limit for one- and two-dimensional (1D and 2D) NEMSs. Indeed, single-walled nanotubes are ultra-narrow wires whose diameter can be as small as 1 nm; graphene, being a sheet of carbon atoms arranged in a honeycomb lattice, is the thinnest membrane imaginable. Figure 1 shows mechanical devices made from a carbon nanotube and a graphene sheet.

Owing to their reduced dimensionality, graphene and carbon nanotubes display unusual mechanical behavior. We will discuss two examples in the following. The first one concerns the force-displacement response. In the well established case of the cantilever of an atomic force microscope probe, its position changes linearly with the force it is subjected to. Such a linear force-displacement response is also found in doubly-clamped beams (see Fig. 2a and

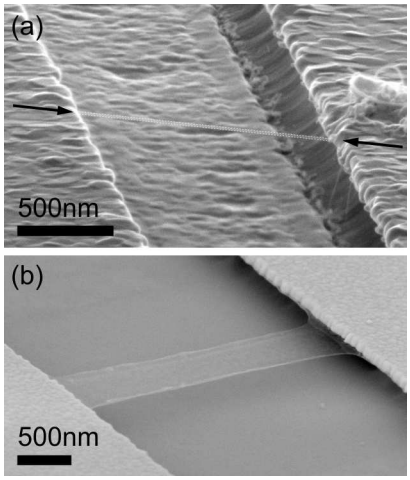

FIG. 1: (a) Scanning electron microscopy image of a nanotube resonator. The nanotube was grown by chemical vapor deposition over a prefabricated trench between two W/Pt contacts. The nanotube is marked by the arrows and the white dotted lines. (b) Scanning electron microscopy image of a suspended single-layer graphene sheet with Au contacts. (Adapted with permission from Ref.[25].)

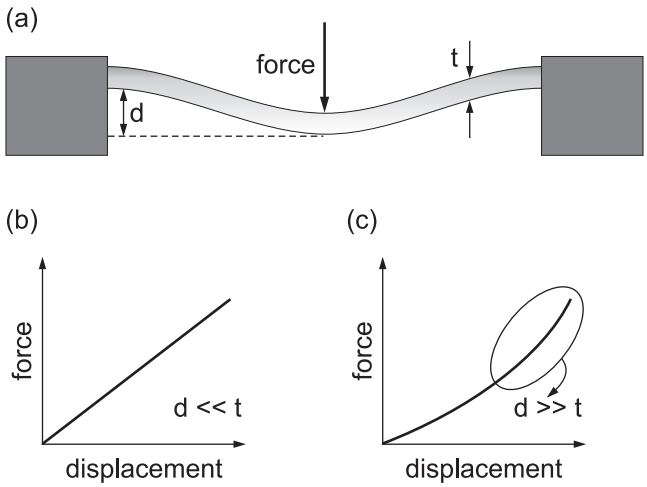

FIG. 2: (a) Schematic of a suspended beam clamped at both ends and subject to a force. (b,c) Expected force-displacement characteristics when the displacement d is much lower than the beam thickness t (b) and when d is much larger than t (c).

b). According to continuum elasticity theory, in the latter case this linearity is expected to hold only when the displacement is much smaller than the thickness of the beam[26]. Because the diameter of a nanotube and the thickness of a graphene sheet are usually both small compared to any displacement, force-displacement measurements in nanotubes and graphene are expected to be highly nonlinear (such as in Fig. 2c). This was indeed shown to be the case for graphene[27].

Another striking example of an unusual mechanical property originating from the reduced dimensionality of these carbon-based resonators concerns the bending rigidity. This quantity characterizes the resistance of an object to bending. Figure 3a shows that the lower region of a bent beam contracts while the upper region expands (when the beam bends upwards). At the microscopic level, the separation between atoms is larger (smaller) in the upper (lower) region. This is energetically not favorable, so the beam tends to return to its initial, straight configuration. In this respect, the case of graphene is intriguing (Fig. 3b): because it is only one atom thick, the bending rigidity results solely from the energy cost of changing the angle between the p_z orbitals of carbon atoms[28]. Thus the microscopic origin of the bending rigidity of graphene differs from the one of standard materials. This book chapter focuses on graphene and nanotube NEMS resonators and on the peculiar mechanical properties that their reduced dimensionality entails.

From a practical point of view, the low dimension and the corresponding ultra-low mass of nanotubes and graphene present a great advantage in such experiments as inertial mass sensing and the exploration of the quantum regime of a macroscopic mechanical degree of freedom. The working principle of mass sensing is simple. Electromechanical resonators can be described as harmonic oscillators with an effective mass m (close to the real mass of the resonator volume), a spring constant k, and a mechanical resonant frequency $f_0 = 1/2\pi \cdot \sqrt{k/m}$. Mass sensing consists in monitoring the shift in f_0 induced by the adsorption of atomic species onto the resonator. The reason for the high mass sensitivity of nanotube resonators is that the mass of a nanotube is ultra-low, so even a tiny amount of atoms deposited on the nanotube makes up a significant fraction of the total mass. Whence, it has been possible to achieve a mass sensitivity of about 1 zg $= 10^{-21}$ g with a nanotube resonator[8–10], which surpasses the sensitivity achieved using resonators based on other materials[29]. Note that the frequency shift in inertial mass sensing depends not only on the adsorbed mass but also on the position of the adsorbate. By exploiting the nonlinear mechanics of nanoscale resonators, the position can in principle be determined by a measurement at the fundamental resonant frequency by using a multi-frequency excitation scheme[30].

Their low mass makes carbon nanotubes and graphene very promising for the study of their motion in the quantum regime. This in practice requires preparing the resonator mode (oscillator) close to its quantum ground state. What makes such experiments a technological feat is that the amplitude of the zero-point motion is typically very low ($x_{zp} = \sqrt{\hbar/4\pi f_0 m}$), and therefore difficult to detect. In this context, graphene and nanotubes offer the immediate advantage of a very low mass that renders the zero-point motion larger than in heavier resonators. A ballpark figure for x_{zp} is typically $1 - 10$ fm for resonators microfabricated from semiconducting and metallic materials and operated in the $1 - 10$ MHz range[31,32]. By contrast, x_{zp} is expected to be $1 - 10$ pm for graphene resonators with similar resonant frequencies. Not only does a large zero-point motion make detecting the motion in the quantum limit easier, it also allows for an enhanced coupling to other degrees of freedom, such as the photons of a superconducting resonator[31,32] and the qubit in a Cooper-pair box[33]. This coupling to nonlinear elements such as two level systems is needed to observe quantum dynamics; interestingly, however, graphene resonators are nonlinear at very small oscillation amplitudes, opening the possibility to study quantum dynamics without external components[34]. We note that the quantum dynamics of nonlinear vibrations was investigated

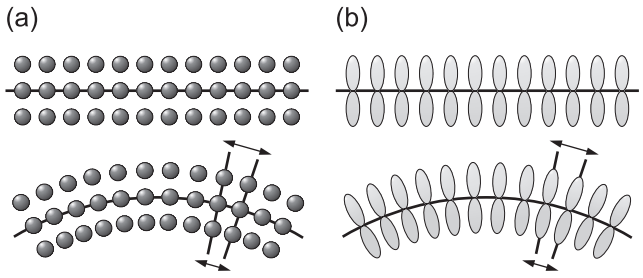

FIG. 3: (a) Arrangement of the atoms of a beam in a straight (top) and bent (bottom) geometry. (b) Arrangement of the p_z electronic orbitals of the carbon atoms of a graphene sheet in a straight (top) and bent (bottom) geometry. The bending energy is given by the energy cost for the electronic orbitals to rotate.

in the past by means of spectroscopy measurements of the vibrations of impurities in solids[35].

II. DETECTION OF THE MECHANICAL VIBRATIONS

Even though carbon nanotubes and graphene are outstanding materials for NEMS resonators, what first hindered progress in this research field is the difficulty to detect their mechanical vibrations. Nanotubes and graphene are so small that it is challenging to apply the detection schemes used for larger mechanical resonators[36]. The first measurements were carried out by transmission and scanning electron microscopy[1,4] as well as field emission[3], but these detection schemes are suitable neither for sensing nor for experiments in the quantum limit. Over the last few years, efforts have been made to develop new detection schemes based e.g. on optical interferometry[18], atomic force microscopy[7,19], electrical[11], and capacitive[37,38] readouts. A technique that has become very popular is the mixing technique. It essentially consists of measuring the electrical current flowing through the graphene sheet or the nanotube. This detection scheme is very practical since it can be implemented in various experimental setups, such as cryostats and ultra-high vacuum chambers. The method was first used in experiments on microfabricated resonators[39] and was later on adapted to nanotube resonators by the McEuen group at Cornell[5]. The mixing technique was recently improved by the group in Lyon[14] and we will discuss this improved version.

The resonator is actuated electrostatically by applying an oscillating voltage V^{FM} with amplitude V^{AC} to the source electrode, which creates an alternating potential between the

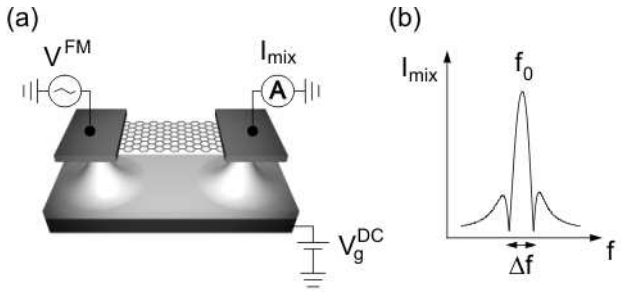

FIG. 4: (a) Schematic of the device layout and the actuation/detection setup. (b) Schematic of the frequency response of the mixing current. The separation between the two minima corresponds to the resonance width Δf, equal to f_0/Q. (Adapted with permission from Ref.[25].)

resonator and the gate electrode (Fig. 4a). Central to the technique is the fact that this driving voltage is frequency modulated (FM) to take the form $V^{FM} = V^{AC}\cos[2\pi f t + f_\Delta/f_L \cdot \sin(2\pi f_L t)]$, where f is the carrier frequency and f_Δ is called frequency deviation. The motion is detected by measuring the current at frequency f_L at the drain electrode, $I_{\rm mix} \propto |\partial {\rm Re}[x_0]/\partial f|$, where ${\rm Re}[x_0]$ is the real part of the frequency response function of the displacement x_0. The expression $|\partial {\rm Re}[x_0]/\partial f|$ can be understood as follows. It contains an absolute value because $I_{\rm mix}$ is measured with a lock-in amplifier and the output signal is the module of the current. The derivative with respect to f is a consequence of the modulation of the applied voltage: V^{FM} can be seen as an oscillating voltage whose frequency is modulated as $f_i = f + f_\Delta \cos(f_L t)$ (valid over a timescale shorter than Q/f_0, where Q is the quality factor and f_0 the resonant frequency of the mechanical resonator). Finally, the origin of the real part in $|\partial {\rm Re}[x_0]/\partial f|$ is less transparent; as shown in[14], it comes from the Taylor expansion of $I_{\rm mix}$ at small motional amplitude $\delta x(t)$ and small drive voltage $\delta V(t)$, whose only component at frequency f_L is contained in the term $\partial^2 I_{\rm mix}/\partial x \partial V \cdot \delta x \delta V$.

One advantage of this measurement technique is the frequency conversion. The frequency of the measured signal (f_L) is about 1 kHz whereas the motion of the resonator can have much higher frequencies (typically $10 - 1000$ MHz). This frequency conversion is essential since the impedance of nanotube and graphene resonators is much larger than 50 Ohm, which makes it difficult to measure small high-frequency currents through the resonator. A further advantage of this detection scheme is that the mixing current as a function of f has a characteristic line-shape (Fig. 4b), which allows us to extract the mechanical quality

factor Q in a simple manner: the resonance peak at frequency f_0 is flanked by two minima whose separation is the resonance width $\Delta f = f_0/Q$ for a linear harmonic oscillator. Later on we will see that the distance between these two minima is also a natural measure of Q in a nonlinear oscillator.

Choosing the right value for the frequency deviation (f_Δ) of the FM technique is crucial for a reliable measurement. Namely, one has to ensure that f_Δ is sufficiently small compared to the width of the mechanical resonance Δf (typically, $f_\Delta < \Delta f/4$). Otherwise, the measured resonance broadens[14,25]. (In practice, we measure the dependence of Δf on f_Δ; the real resonance width is obtained at low f_Δ where Δf saturates).

III. VARIATION OF THE QUALITY FACTOR WITH THE AMPLITUDE OF THE MOTION

Large mechanical resonators, such as those microfabricated from metallic or semiconducting materials, are usually well described as simple harmonic oscillators. The equation of motion is then given by the well-known expression:

$$md^2x/dt^2 = -kx - \gamma dx/dt + F_{\rm drive}\cos(2\pi ft) \qquad (1)$$

which interrelates the position x, the velocity dx/dt, and the acceleration d^2x/dt^2 of the oscillator (with effective mass m, spring constant k, and damping rate γ). Here, we show that the motion of graphene/nanotube resonators is different from that of larger mechanical resonators[25]. The most striking difference is that the damping depends on the amplitude of the motion, in sharp contrast to the behavior of simple harmonic oscillators.

A surprising experimental fact in nanotube and graphene resonators is that the mechanical resonance lineshape often broadens as the driving force is increased ($F_{\rm drive} = C'V_g^{DC}V^{AC}$ where C' is the derivative of the gate-resonator capacitance with respect to x). In other words, the quality factor depends on the amplitude of the motion. This is a novel phenomenon: indeed, in larger resonators the quality factor is independent of the motional amplitude ($Q = 2\pi f_0 m/\gamma$).

Figure 5a shows an example of the variation of the resonance width (and of the quality factor on the right axis) as a function of driving force (which scales linearly with V^{AC}) in a logarithmic plot. The variation of the quality factor is significant and can reach a factor

of 50 for some devices. This behavior is robust as it can be observed both in nanotube and graphene resonators, both at low temperature (down to 90 mK) and at room temperature, and using different detection methods (namely, the FM method described in the previous section, the so-called two source technique[5], and optical interferometry[18]).

The dependence of the mechanical quality factor on the amplitude of the driving force came as a surprise to us. A single mention of this phenomenon appears in[18], but its origin is not discussed. One possible reason why this effect remained unnoticed before is that the variation of the quality factor becomes clearly visible only over a rather large span of driving force amplitudes, while the detection of the motion at low drive is challenging. In these

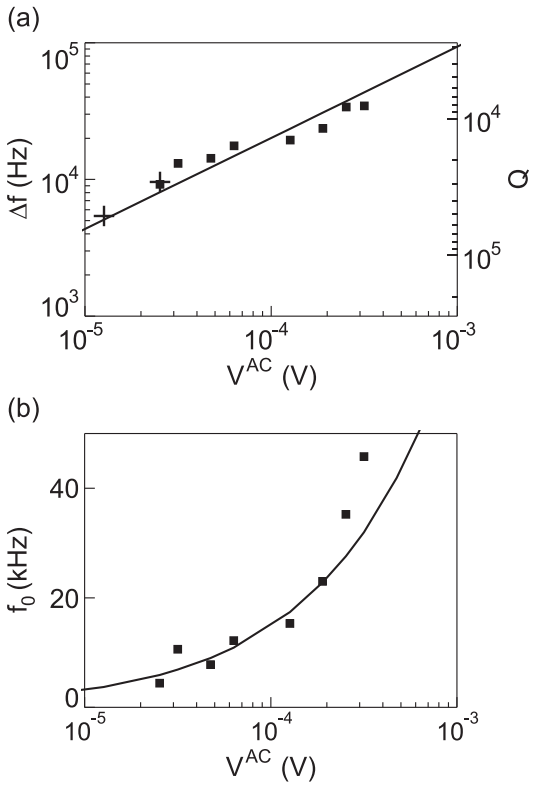

FIG. 5: Measurements of the mechanical properties of a resonator made from a nanotube under tension. The length of the nanotube is 840 nm and the radius is 2 nm. (a) Resonance width as a function of drive V^{AC}. Squares correspond to 5 K and crosses to 400 mK. The line corresponds to equation (5) with $\eta = 10^4$ kg·m$^{-2}\cdot$s^{-1} ($\gamma = 0$). The corresponding quality factor Q is shown on the right-hand side scale. (b) Resonance shift as a function of V^{AC}. The line is a solution to equation (3) with $\alpha = 6\cdot 10^{12}$ kg·m$^{-2}\cdot$s^{-2}. (Adapted with permission from Ref.[25].)

measurements, care is taken to avoid driving V^{AC} above $k_{\mathrm{B}}T/e$ in order to prevent electronic nonlinear effects or local heating (here k_{B} is the Boltzmann constant, T the temperature, and e the electron charge). (On a technical note, the variation of the quality factor does not stem from the coupling between electrons and mechanical vibrations[12,13] because the effect is not associated to Coulomb blockade and V^{AC} is kept below $k_{\mathrm{B}}T/e$, see Ref.[25] for a more detailed discussion.)

In order to understand the variation of the quality factor with the drive, it is useful to first discuss another behavior. Increasing the driving force also shifts the resonant frequency to higher (or sometimes lower) values (Fig. 5b). This behavior is usually associated to the so-called Duffing force $F_{\mathrm{Duffing}} = -\alpha x^3$ (Ref.[40]). The latter, together with the spring force, can be expressed as

$$-k\left(1+\frac{\alpha}{k}x^2\right)x \tag{2}$$

which indicates that the Duffing term contributes to the restoring force: it makes the resonator stiffer (for $\alpha > 0$) and increases the resonant frequency. However, the Duffing force alone cannot explain the variation of the quality factor with drive, since it does not affect the resonance width (in the absence of any bistability), provided that the amplitude of thermal fluctuations is smaller than that of the driven motion[41]. This is readily verified by adding the Duffing force to the right hand side of equation (1) and solving for the steady state. The resonance width, given by the separation between the two minima in the mixing current as a function of f in the FM technique, is indeed independent of the driving force. In addition to the Duffing nonlinearity $-\alpha x^3$, the other relevant higher-order term in the Newton equation for a weakly anharmonic oscillator is the nonlinear damping term $-\eta x^2 dx/dt$ (Ref.[40,42,43]). We thus get

$$md^2x/dt^2 = -kx - \gamma dx/dt - \alpha x^3 - \eta x^2 dx/dt + F_{\mathrm{drive}}\cos(2\pi f t) \tag{3}$$

A derivation of equation (3) based on the Caldeira-Leggett model can be found in[43], in which the nonlinear damping force emerges from a nonlinear coupling between the mechanical resonator and a thermal bath of harmonic degrees of freedom (the nonlinearity in the coupling results from the anharmonicity of the potential well in which the resonator is confined). Other works showed that additional terms of second and third order (x^2, xdx/dt, $(dx/dt)^2$, $x(dx/dt)^2$, $(dx/dt)^3$) lead in the rotating frame to a renormalization of α and η (Ref.[40–42]).

The term $-\eta x^2 dx/dt$ is a damping force since it scales linearly with the velocity. Together with $-\gamma dx/dt$, it can be expressed as

$$-\gamma\left(1+\frac{\eta}{\gamma}x^2\right)dx/dt \tag{4}$$

The force $-\eta x^2 dx/dt$ accounts for a dissipation mechanism that becomes important at large motional amplitude. When $-\gamma dx/dt$ dominates over $-\eta x^2 dx/dt$, which is the case for larger mechanical resonators, the resonance width is independent of the driving force and is given by $\Delta f = \gamma/2\pi m$. In the opposite limit[25], when the term $-\gamma dx/dt$ can be neglected,

$$\Delta f = 0.032 m^{-1}\eta^{1/3} f_0^{-2/3} F_{\rm drive}^{2/3} \tag{5}$$

so that $\Delta f \propto (V^{AC})^{2/3}$. At first sight, the simple relation $Q = f_0/\Delta f$ for a linear harmonic oscillator is expected to break down in the presence of nonlinearities. However, we show in[25] that an analogous expression $Q = 1.09 f_0/\Delta f$ is recovered in the limit of strong nonlinear damping.

The relation $\Delta f \propto (V^{AC})^{2/3}$ captures well the experimental data: the line in the double logarithmic plot of Fig. 5a corresponds to a power law with an exponent 2/3. This fit allows to extract η. The agreement between experiment and theory is a strong indication that damping is here described by the nonlinear force $-\eta x^2 dx/dt$, instead of the linear force $-\gamma dx/dt$.

In the following we discuss two additional experimental facts which further support the dominance of the nonlinear damping force in nanotube/graphene resonators. These are revealed by studying the hysteretic behavior of the mechanical resonance on one hand and parametric excitation on the other.

IV. HYSTERESIS

For sufficiently large driving forces, the motional amplitude as a function of the driving frequency f develops an asymmetry (dashed line in Fig. 6a, b). This results in bistability and hysteresis for certain intervals in f (solid line in Fig. 6a, b)[5,21]. The hysteresis is intimately related to the resonance shift and also originates from the Duffing force[40,44–46]. An example of a hysteretic resonance lineshape for a graphene resonator is shown in Fig. 6c, d. Surprisingly, however, we do not observe a hysteresis in some of our nanotube and

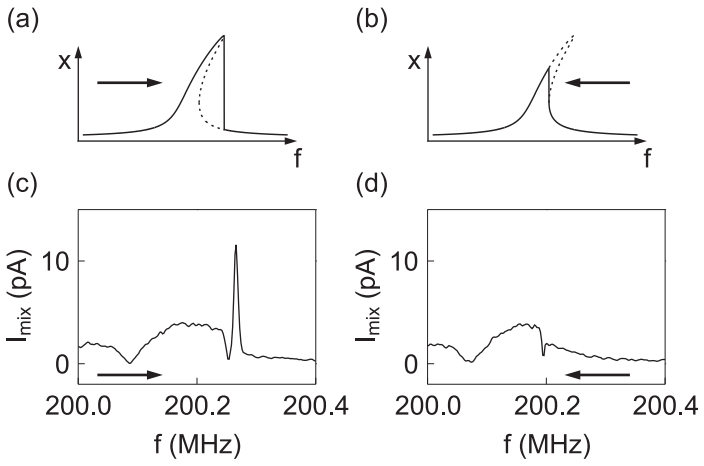

FIG. 6: Mechanical properties of a resonator made from a graphene sheet under tensile stress at 4 K for large driving forces. The length of the sheet is 1.7 μm and the width is 120 nm. (a, b) The schematics show the amplitude of motion as a function of driving frequency (solid lines) for both sweeping directions. The dashed lines are the solutions of the Duffing equation. (c, d) Frequency response of the mixing current at $V^{AC} = 500$ μV. The frequency is swept upwards in (c) and downwards in (d). (Adapted with permission from Ref.[25].)

graphene resonators. This is particularly intriguing since hysteretic behaviors are always observed in larger mechanical resonators.

The occasional absence of hysteresis is a direct consequence of nonlinear damping. It can be predicted from the ratio between the constants of the nonlinear forces α and η. When $\eta/\alpha > \sqrt{3}/2\pi f_0$, the nonlinear damping is strong enough to keep the broadening of the resonance always comparable to or larger than its shift and precludes hysteresis for all driving forces[40]. In the opposite case (when $\eta/\alpha < \sqrt{3}/2\pi f_0$), a hysteretic behavior is expected to emerge.

In the previous section we saw how η can be extracted from the drive dependence of the quality factor. The parameter α is evaluated by fitting the shift of the resonant frequency as a function of V^{AC} to the steady-state solution of equation (3) (see solid line in Fig. 5b). By comparing η/α to $\sqrt{3}/2\pi f_0$, we can predict the occurrence of the hysteresis. The agreement between experiment and theory is good in most cases. This provides the second experimental fact that supports the relevance the nonlinear damping force.

V. PARAMETRIC EXCITATION

A whole new range of interesting effects becomes accessible by modulating the parameters that enter the Newton equation. For example, nonlinear experiments can be carried out by periodically modulating the spring constant $k + \delta k \cos(2\pi f_p t)$. In the case of a pendulum, the spring constant can be changed by varying the length of the pendulum's arm (Fig. 7a). The pendulum can then be brought to resonance by setting f_p to be an integer multiple of f_0, while keeping the driving force to zero. This is what we refer to as "parametric excitation".

Nanotube resonators are expected to be excellent candidates for parametric excitation because k can be modulated with the voltage applied to the gate by a very large amount: it is possible to make this modulation larger than in any other mechanical resonators fabricated to date (this can be quantified by measuring the gate voltage dependence of the resonant frequency, which scales as $\sqrt{k}$). Figure 7b shows two clearly resolved resonant modes. Their resonant frequency can be tuned with V_g^{DC} to a large extent. This behavior has been attributed to the increase of the elastic tension that builds up in the nanotube as it bends

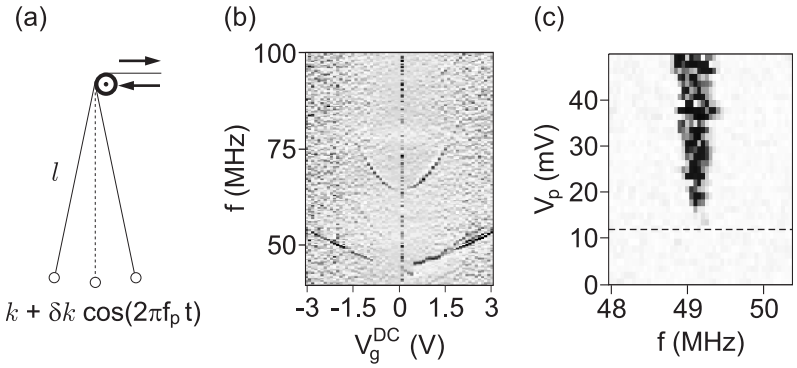

FIG. 7: (a) Schematic of a pendulum. By periodically modulating the length l, one also modulates the spring constant $k + \delta k \cos(2\pi f_p t)$ with f_p an integer number of the resonant frequency f_0 ($k = mg/l$, where m is the mass of the pendulum and g is the constant of gravitation). In so doing, the pendulum can be brought to resonance. (b) Resonant frequency as a function of gate voltage (data obtained by measuring I_{mix} versus f and V_g^{DC}). Two mechanical modes can be seen. (c) Parametric excitation signal (dark) obtained by measuring I_{mix} as a function of the detection frequency f and V_P. The phase difference between V_P and V_{sd}^{AC} (the drive signal) is not kept fixed so the measured I_{mix} is fluctuating. $V_{sd}^{AC} = 1.4$ mV. (Adapted with permission from Ref.[17]).

towards the gate with increasing V_g^{DC} (Ref.[5]), in a similar fashion as a bent guitar string vibrates at higher frequency.

In order to realize parametric excitation, we apply an oscillating voltage V_P at a frequency $2f$ to the gate electrode (another excitation scheme has recently been proposed by some of us[47] and consists in applying a symmetric source-drain voltage). On resonance, this modulates k at $2f_0$, thereby achieving parametric pumping of the resonator. The resulting motion is detected using the so-called two-source technique[5], that is, by applying a small voltage V_{sd}^{AC} at a slightly detuned frequency $(f - \delta f)$ to the source electrode, and by measuring the mixing current $I_{\rm mix}$ at frequency δf at the drain electrode using a lock-in amplifier.

Upon increasing the parametric pump excitation above a critical threshold $V_{P,C}$, the nanotube is observed to oscillate without any driving force (Fig. 7c). The resonator becomes unstable, so that any fluctuation will activate an oscillating motion that is sustained by the parametric drive[40]. Figure 7c shows mechanical motion in a tongue-shaped region of the (f, V_P) space, which is a typical signature of self-oscillation[40,48–52]. Self-oscillation is observed for V_P roughly above $V_{P,C} = 10$ mV. In[17] we describe additional measurements (parametric amplification measurements) of the same device, which independently yields $V_{P,C} \simeq 10$ mV.

One interesting outcome of this experiment is that the estimation of $V_{P,C}$ allows to extract the constant γ of the linear friction force $-\gamma dx/dt$ and the associated quality factor $Q_0 = 2\pi f_0 m/\gamma$ since below threshold the motional amplitude is so small that nonlinear damping can be neglected. Here, we use the simple relation

$$Q_0 = \frac{1}{V_{P,C}} \cdot \frac{f_0}{df_0/dV_g^{DC}} \tag{6}$$

where df_0/dV_g^{DC} is the slope of the V_g^{DC} dependence of f_0, and obtain a quality factor $Q_0 \simeq 1000$. This is significantly larger than the quality factor obtained when the parametric pump excitation is off (where the quality factor is extracted from the resonance lineshape of the resonator driven by $F_{\rm drive}\cos(2\pi f t)$). There, the quality factor is about $170 - 350$ depending on the driving force (as in section III). We attribute this difference to the distinct damping forces at work: $-\gamma dx/dt$ and $-\eta x^2 dx/dt$. While $V_{P,C}$ extracted from parametric excitation measurements is a measure of γ, the main damping channel is associated to the force $-\eta x^2 dx/dt$. This is an additional experimental fact in favor of the nonlinear damping scenario in nanotube and graphene resonators.

VI. DISCUSSION ON THE NONLINEAR DAMPING FORCE

We have shown that the dynamics of graphene and carbon nanotube mechanical resonators is highly unusual: the quality factor depends on the amplitude of the motion. We emphasize however that the quality factor can in principle saturate at low driving force for the two following reasons. First, the quality factor is expected to be independent of the driving force when the amplitude of thermal vibrations is much larger than that of the driven motion, even if the damping is dominated by the $-\eta x^2 dx/dt$ force (M. Dykman, private communication). Owing to the small mass of nanotubes and graphene sheets, the amplitude x_{th} of the thermal vibrations is large. Using

$$x_{th} = \frac{1}{2\pi f_0}\sqrt{\frac{k_{\rm B}T}{m}} \tag{7}$$

yields $x_{th} = 1.4$ nm at 300 K for a nanotube with $f_0 = 100$ MHz and $m = 5$ ag (which is the mass of a nanotube 1 μm in length and 2.2 nm in diameter). The amplitude of the vibrations of driven nanotube resonators was estimated from the measurements to be typically $1 - 10$ nm at room temperature[5,6,17]. As such, the quality factor is expected to rapidly saturate at 300 K at low driving forces (even if the linear therm $-\gamma dx/dt$ is negligible).

Naturally, a second mechanism that leads to the saturation of the quality factor at low drive is the crossover from a nonlinear to a linear damping regime. Provided that Δf and the resonance shift are much smaller than f_0, the standard definition of Q is still warranted and reads $Q = 2\pi E/\Delta E$ where ΔE is the mechanical energy dissipated over one oscillation period and E is the corresponding stored energy when the resonator is driven resonantly. We obtain

$$1/Q = \frac{\gamma}{2\pi f_0 m}\left(1 + \frac{\eta}{4\gamma}x_0^2\right) \tag{8}$$

which shows that the quality factor depends on the driving force at large x_0 whereas it becomes a constant at low x_0 (here, x_0 is the maximum steady state amplitude on resonance).

Figure 8 shows that the quality factor of a nanotube resonator measured at 300 K saturates at low driving force. The dashed line is a fit to the model that assumes the occurrence of a crossover from the nonlinear to the linear damping regime using γ and η as fit parameters (we note that the device is different from that in Fig. 5). We emphasize that the data can alternatively be captured by a model that assumes that the saturation is due to the

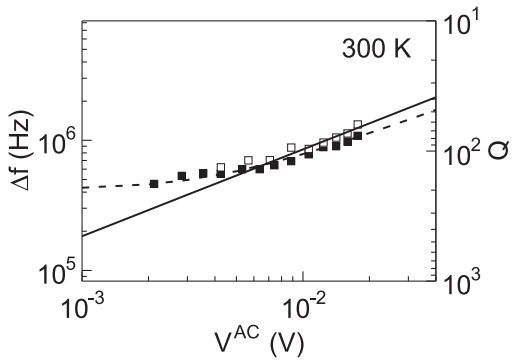

FIG. 8: Measurements of the mechanical properties of a resonator made from a nanotube at 300 K. Resonance width and quality factor as a function of driving force measured with the FM technique (filled squares) and 2-source technique (hollow squares), respectively. The solid line represents a comparison to equation (5) with negligible linear damping ($\eta = 2.5 \cdot 10^3$ kg·m$^{-2} \cdot$ s^{-1}, $\gamma = 0$), the dashed line is obtained with a finite γ ($\eta = 1 \cdot 10^3$ kg·m$^{-2} \cdot$ s^{-1}, $\gamma = 1.9 \cdot 10^{-14}$ kg·s^{-1}). (Adapted with permission from Ref.[25].)

thermal vibrations. More work is required to identify the proper contributions of each of these two effects.

The theoretical foundations of damping rest on Newton's Principia. Damping has been successfully described by the linear damping force $-\gamma dx/dt$ for all mechanical resonators studied so far in vacuum. Remarkably, this picture holds for resonators whose dimensions span many orders of magnitude down to a few tens of nanometers. Reducing dimensions to the atomic scale using graphene and nanotube resonators, our work demonstrates that the simple linear damping scenario ceases to be valid and damping is often better described by incorporating $-\eta x^2 dx/dt$.

This finding has profound consequences in light of the fact that several predictions regarding quantum and sensing experiments assume that damping is linear. Such experiments, if carried out with nanotube or graphene resonators, would indeed have to be interpreted within the framework of nonlinear damping. These include studies of the quantum-to-classical transition[53], the cooling efficiency[54], the mass resolution[55], and the force sensitivity[56].

Our results not only provide new insight into the dynamics of nanotube and graphene resonators, they also hold promise for technological applications. Our control over the res-

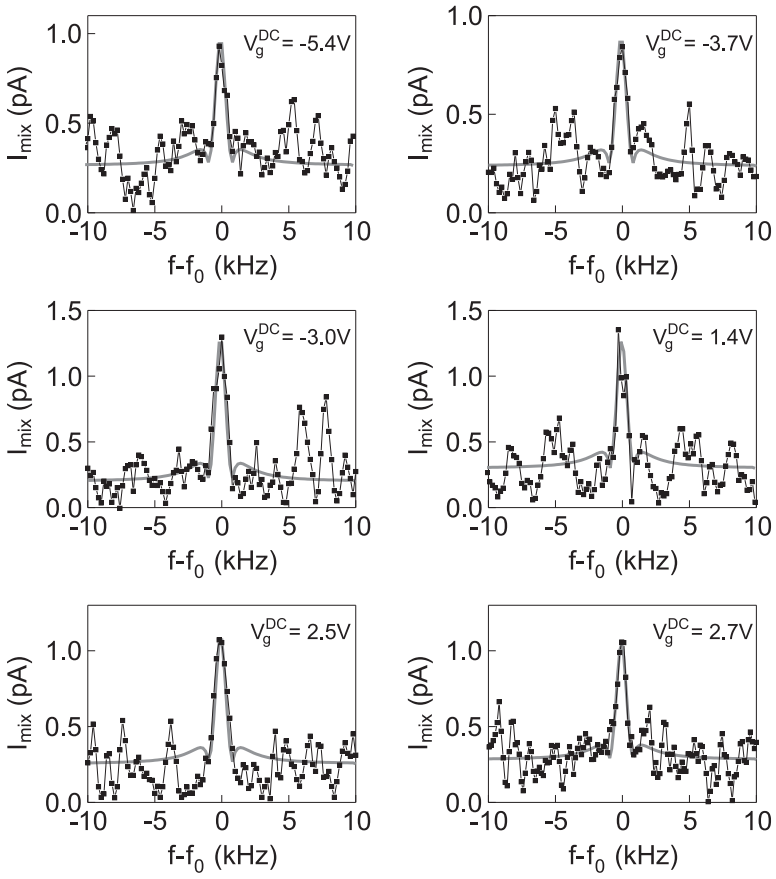

FIG. 9: Frequency response of the mixing current for a graphene resonator. Each panel corresponds to a given gate voltage. The solid lines are fits with $Q = 10^5$. Measurements are carried out at 90 mK with $V^{AC} = 8$ μV. The integration time of the lock-in amplifier is 300 ms. $f_\Delta = 1$ kHz and similar results are obtained with $f_\Delta = 500$ Hz. The resonance width is typically 1.5 kHz (and occasionally 300 Hz smaller or larger). (Adapted with permission from Ref.[25].)

onance width allows us to improve the mechanical quality factor. In order to achieve larger Q-factors, we simply lower the driving force until the motion becomes barely detectable. For this, it is convenient to select the value of V_g^{DC} for which the detection signal is largest. In so doing, we measured a quality factor of 10^5 for a graphene resonator at 90 mK (see Fig. 9), which is the largest Q ever reported in a graphene resonator[25]. Larger quality factors enable better force sensing. We obtained a force sensitivity of 2.5 aN/$\sqrt{\text{Hz}}$ using a nanotube resonator operating at 100 mK. This is within a factor of five of the best sensitivities reported using microfabricated resonators operating at their ultimate limit set by thermal vibrations[57,58].

The microscopic origin of the nonlinear damping is still to be determined, but it could be related to such diverse phenomena as phonon tunneling into the supports[59,60], sliding at the contacts, nonlinearities involving phonon-phonon interactions, or contamination in combination with geometrical nonlinearities[25]. It would be of considerable interest to experimentally study the dependence of the nonlinear damping force on contamination, the clamping configuration, and the suspended length. Theoretical work on the microscopic nature of nonlinear damping should also prove valuable[42,43].

VII. COUPLING MECHANICAL VIBRATIONS TO ELECTRON TRANSPORT IN A NANOTUBE RESONATOR

Lastly, we show that strong electromechanical nonlinearities arise when a nanotube resonator operated in the Coulomb blockade regime vibrates in concert with single electron hopping.

Figure 10 shows the mechanical properties of a nanotube resonator at 4 K. Both the resonant frequency and the quality factor oscillate as a function of the voltage applied to the backgate electrode. These measurements show that the dynamics of nanotubes can be widely tuned by external electric means (V_g^{DC}), which is very advantageous for applications.

To understand the origin of the oscillations of the resonant frequency and of the quality factor, it is useful to first consider the electrical properties of the nanotube. The conductance oscillates with V_g^{DC} in a way that is typical of the Coulomb-blockade regime and with the same V_g^{DC} period as the oscillations of f_0 and Q (see Ref.[12]). This correlation indicates that the mechanical motion is affected by Coulomb blockade.

Charge transport through nanotubes in the Coulomb-blockade regime is a well-studied phenomenon. Upon sweeping V_g^{DC}, the conductance oscillates as the charge $q_{\rm dot}$ residing on the nanotube increases stepwise (Fig. 11). Furthermore, in our experiment the nanotube behaves as a mechanical resonator. The capacitance C_g between the nanotube and the gate oscillates in time as $\delta C_g = C_g' x$ (with C_g' the derivative of C_g with respect to displacement x). As a result, the nanotube is periodically charging and discharging by the amount $\delta q_{\rm dot} = \delta C_g V_g^{DC}$ (as shown in Fig. 11).

The oscillating charge on the nanotube results in a shift of the resonant frequency of the resonator. When electrons tunnel onto and out of the nanotube, the relevant electrostatic

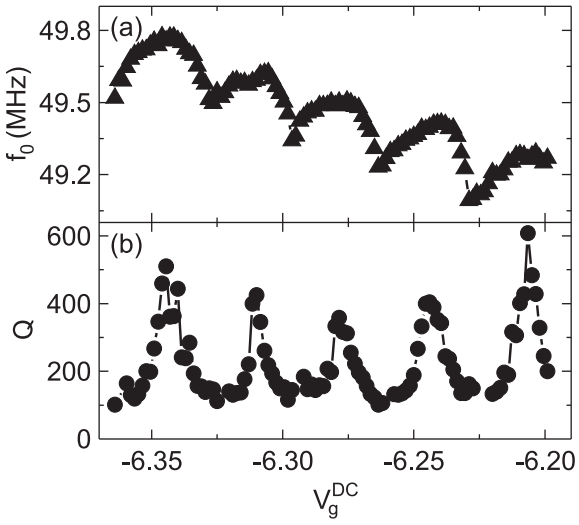

FIG. 10: (a) Resonant frequency and (b) quality factor as a function of gate voltage V_g^{DC} for a nanotube resonator at 4 K. The nanotube length is 1 μm and the diameter is $\sim$ 1.1 nm. (Adapted with permission from Ref.[12].)

force acting on the nanotube can be expressed as[12]

$$F_e = -\frac{C_g' V_g^{DC}}{C_{\rm dot}} \left(q_{\rm dot} - q_{\rm c}\right) \tag{9}$$

where $q_{\rm c} = -C_g V_g^{DC}$, called control charge, is introduced for commodity (this force comes from $F_e = 0.5 C_g'(V_{\rm dot} - V_g^{DC})^2$ with the electrostatic potential of the nanotube dot $V_{\rm dot} = (q_{\rm dot} - q_{\rm c})/C_{\rm dot}$). Because of the repeated charging and discharging of the nanotube by the amount $\delta q_{\rm dot}$, equation (9) results in a spring force, $F_e = -\delta k \cdot x$. This force modifies the spring constant of the nanotube resonator by δk. As a result, the resonator softens and the resonant frequency gets reduced by the amount $\delta f_0 = (f_0/2) \cdot (\delta k/k)$.

Besides, charging and discharging the nanotube causes damping of the mechanical motion. Indeed, the charge $\delta q_{\rm dot}$ has to flow across the tunnel barrier at the nanotube-electrode interface, and the dissipated energy of the charge (after the tunnel process) is supplied from the mechanical resonator.

This damping and the resonant frequency are expected to oscillate with V_g^{DC}, since the amplitude of the $\delta q_{\rm dot}$ oscillations depends on V_g^{DC}. The amplitude is large (low) when $q_{\rm dot}$ increases sharply (weakly) with V_g^{DC}; see Fig. 11. Our model captures the data well as discussed in[12]. We note that the background signal of the resonant frequency in Fig. 10a decreases continuously over the full V_g^{DC} sweep: this is attributed to the increase of the

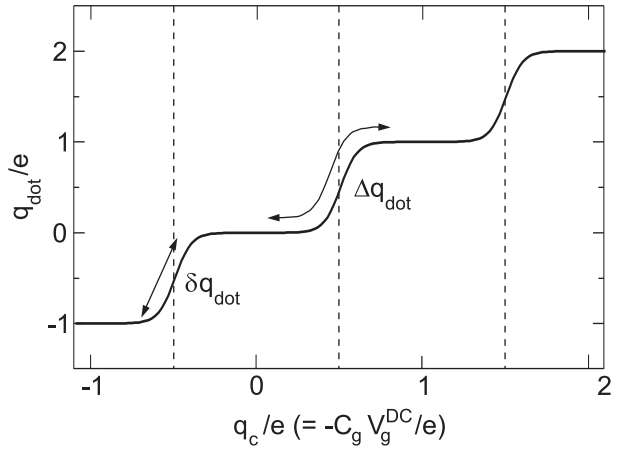

FIG. 11: Schematic of the charge on the nanotube dot as a function of the control charge ($q_c = -C_g V_g^{DC}$) in the Coulomb-blockade regime. Vibrations cause the charge on the nanotube to oscillate (with amplitude $\delta q_{\rm dot}$ and $\Delta q_{\rm dot}$ for low and large motional amplitude, respectively). (Adapted with permission from Ref.[12].)

elastic tension that builds up in the nanotube as it bends towards the gate upon increasing V_g^{DC}[5]. Second, the (oscillating) dips of the resonant frequency in Fig. 10a are not symmetric, which may be caused by the stepwise change of the electrostatic potential when sweeping V_g^{DC} (Ref.[13]).

As we have seen, the coupling between mechanical vibrations and charge transport results in an electrostatic force acting on the nanotube[12]

$$F_{\rm electro} = -k_{\rm electro} x - \gamma_{\rm electro} dx/dt \tag{10}$$

where the constants $k_{\rm electro}$ and $\gamma_{\rm electro}$ can be tuned with V_g^{DC}, which is very practical for future use. $\gamma_{\rm electro}$ is so large that the associated damping force dominates over the $-\eta x^2 dx/dt$ force. Equation (9) is valid for low $\delta q_{\rm dot}$. The situation changes for large mechanical oscillation amplitude. The charging and discharging of the dot becomes highly non-trivial during one oscillation cycle (see $\Delta q_{\rm dot}$ in Fig. 11). As a result, $F_{\rm electro}$ is expected to depend non-linearly on x and dx/dt (in contrast to the linear dependences at low oscillation amplitude) and $F_{\rm electro}$ has to be solved numerically[12].

We found evidences for nonlinearities in $F_{\rm electro}$. Figures 12a,b show two resonance peaks at 1.5 K (mixing current as a function of driving frequency measured using the two-source technique[5]). The resonance in Fig. 12a has a surprising lineshape –it splits into two peaks,

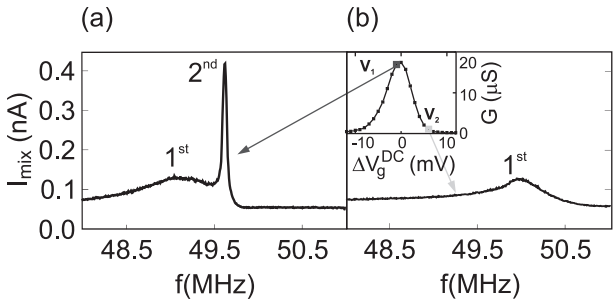

FIG. 12: Mixing current I_{mix} as a function of driving frequency for two different gate voltages at 1.5 K. A second, narrow peak appears in (a). The inset shows the nanotube conductance as a function of gate voltage V_g^{DC}. ΔV_g^{DC} is measured from the maximum of the Coulomb-blockade peak. The nanotube is the same as in Fig. 10. (Adapted with permission from Ref.[12].)

one broad and the other narrow. The narrow peak appears only at gate voltages which yield a Coulomb blockade peak in the conductance (inset of Fig. 12b). Strikingly, its width narrows down as the driving force increases. We show in[12] that the double-peak structure arises from the interplay between two nonlinear phenomena, one associated with the nonlinear force F_{electro} and the other with the nonlinear detection mechanism. Indeed, the nonlinearity in the detection mechanism due to Coulomb blockade can affect the lineshape of the frequency-dependent amplitude $x(f)$ in such a way that the lineshape of $I_{mix}(f)$ develops a double peak structure (the reason for this is that for sufficiently large motional amplitude I_{mix} decreases when x increases)[12]. If the $x(f)$ lineshape were a Lorentzian, the double-peak structure in I_{mix} would be symmetric. However, the nonlinear force F_{electro} renders the $x(f)$ lineshape strongly asymmetric, which results in two peaks in $I_{mix}(f)$, one broad and the other narrow[12].

Overall, these results show that the coupling between mechanical motion and electron transport in nanotube resonators can be made so strong that the associated force acting on the nanotube becomes highly nonlinear in its displacement and velocity. This strong coupling originates from the reduced dimension of nanotubes. Larger and heavier mechanical resonators are evidently much less sensitive to the motion of individual tunneling electrons[12].

We note that this electro-mechanical coupling also influences charge transport in the Coulomb blockade regime, a topic that has attracted much interest[61–74]. Another active field of research consists in harnessing this coupling to cool the mechanical motion of resonators

to the phononic ground state[75–80], as well as controling the dynamics of large cantilevers of scanning probe microscopes[81–86].

VIII. CONCLUSION

Graphene and carbon nanotubes are very interesting systems for studying resonant mechanical behavior. They constitute the ultimate size limit of one and two-dimensional NEMSs: nanotubes are wires with a diameter of about 1 nm and graphene is a membrane that is only one atom thick. Because of their reduced dimensionality, graphene and carbon nanotubes display unusual mechanical phenomena, among which strong nonlinearities are ubiquitous. In this chapter, we reviewed several types of nonlinear behavior. We first discussed an unprecedented scenario where damping is described by a nonlinear force. This scenario is supported by several experimental facts: (i) the quality factor varies with the amplitude of the motion as a power law whose exponent coincides with the value predicted by the nonlinear damping model, (ii) hysteretic behavior (of the motional amplitude as a function of driving frequency) is absent in some of our resonators even for large driving forces, as expected when nonlinear damping forces are large, and (iii) when we quantify the linear damping force (by performing parametric excitation measurements) we find that it is significantly smaller than the nonlinear damping force. We illustrated this chapter with measurements on nanotube resonators but we also observed the experimental facts (i) and (ii) on graphene resonators (see Ref.[25]). We then reviewed parametric excitation measurements on nanotube resonators, an alternative actuation method which is based on nonlinear dynamics. Finally, we discussed experiments where the mechanical motion is coupled to electron transport through a nanotube. The coupling can be made so strong that the associated force acting on the nanotube becomes highly nonlinear with displacement and velocity. Overall, graphene and nanotube resonators hold promise for future studies on classical and quantum nonlinear dynamics.

IX. ACKNOWLEDGEMENTS

We thank M. Dykman for a critical reading of our manuscript.

---

[1] P. Poncharal, Z. L. Wang, D. Ugarte, and W. A. de Heer, Science **283**, 1513 (1999).

[2] B. Reulet, A. Y. Kasumov, M. Kociak, R. Deblock, I. Khodos, Y. B. Gorbatov, V. T. Volkov, C. Journet, and H. Bouchiat, Phys. Rev. Lett. **85**, 2829 (2000).

[3] S. T. Purcell, P. Vincent, C. Journet, and V. T. Binh, Phys. Rev. Lett. **89**, 276103 (2002).

[4] B. Babić, J. Furer, S. Sahoo, S. Farhangfar, and C. Schönenberger, Nano Lett. **3**, 1577 (2003).

[5] V. Sazonova, Y. Yaish, H. Üstünel, D. Roundy, T. A. Arias, and P. L. McEuen, Nature **431**, 284 (2004).

[6] B. Witkamp, M. Poot, and H. S. J. van der Zant, Nano Lett. **6**, 2904 (2006).

[7] D. Garcia-Sanchez, A. S. Paulo, M. J. Esplandiu, F. Perez-Murano, L. Forró, A. Aguasca, and A. Bachtold, Phys. Rev. Lett. **99**, 085501 (2007).

[8] B. Lassagne, D. Garcia-Sanchez, A. Aguasca, and A. Bachtold, Nano Lett. **8**, 3735 (2008).

[9] H.-Y. Chiu, P. Hung, H. W. C. Postma, and M. Bockrath, Nano Lett. **8**, 4342 (2008).

[10] K. Jensen, K. Kim, and A. Zettl, Nature Nanotech. **3**, 533 (2008).

[11] A. K. Hüttel, G. A. Steele, B. Witkamp, M. Poot, L. P. Kouwenhoven, and H. S. J. van der Zant, Nano Lett. **9**, 2547 (2009).

[12] B. Lassagne, Y. Tarakanov, J. Kinaret, D. Garcia-Sanchez, and A. Bachtold, Science **325**, 1107 (2009).

[13] G. A. Steele, A. K. Hüttel, B. Witkamp, M. Poot, H. B. Meerwaldt, L. P. Kouwenhoven, and H. S. J. van der Zant, Science **325**, 1103 (2009).

[14] V. Gouttenoire, T. Barois, S. Perisanu, J.-L. Leclercq, S. T. Purcell, P. Vincent, and A. Ayari, Small **6**, 1060 (2010).

[15] Z. Wang, J. Wei, P. Morse, J. G. Dash, O. E. Vilches, and D. H. Cobden, Science **327**, 552 (2010).

[16] C. C. Wu and Z. Zhong, Nano Lett. **11**, 1448 (2011).

[17] A. Eichler, J. Chaste, J. Moser, and A. Bachtold, Nano Lett. **11**, 2699 (2011).

[18] J. S. Bunch, A. M. van der Zande, S. S. Verbridge, I. W. Frank, D. M. Tanenbaum, J. M.

Parpia, H. G. Craighead, and P. L. McEuen, Science **315**, 490 (2007).

[19] D. Garcia-Sanchez, A. M. van der Zande, A. S. Paulo, B. Lassagne, P. L. McEuen, and A. Bachtold, Nano Lett. **8**, 1399 (2008).

[20] J. T. Robinson, M. Zalalutdinov, J. W. Baldwin, E. S. Snow, Z. Wei, P. Sheehan, and B. H. Houston, Nano Letters **8**, 3441 (2008).

[21] C. Chen, S. Rosenblatt, K. I. Bolotin, W. Kalb, P. Kim, I. Kymissis, H. L. Stormer, T. F. Heinz, and J. Hone, Nature Nanotech. **4**, 861 (2009).

[22] V. Singh, S. Sengupta, H. S. Solanki, R. Dhall, A. Allain, S. Dhara, P. Pant, and M. M. Deshmukh, Nanotechnology **21**, 165204 (2010).

[23] A. M. van der Zande, R. A. Barton, J. S. Alden, C. S. Ruiz-Vargas, W. S. Whitney, P. H. Q. Pham, J. Park, J. M. Parpia, H. G. Craighead, and P. L. McEuen, Nano Letters **10**, 48694873 (2010).

[24] R. A. Barton, B. Ilic, A. M. van der Zande, W. S. Whitney, P. L. McEuen, J. M. Parpia, and H. G. Craighead, Nano Letters **11**, 1232 (2011).

[25] A. Eichler, J. Moser, J. Chaste, M. Zdrojek, I. Wilson-Rae, and A. Bachtold, Nature Nanotech. **6**, 339 (2011).

[26] L. D. Landau and E. M. Lifshitz, *Theory of Elasticity* (Butterworth-Heinemann and Oxford, 1986), 3rd ed.

[27] C. Lee, X. Wei, J. W. Kysar, and J. Hone, Science **321**, 385 (2008).

[28] J. Atalaya, A. Isacsson, and J. M. Kinaret, Nano Lett. **8**, 4196 (2008).

[29] Y. T. Yang, C. Callegari, X. L. Feng, K. L. Ekinci, and M. L. Roukes, Nano lett. **6**, 583 (2006).

[30] J. Atalaya, J. M. Kinaret, and A. Isacsson, Europhys. Lett. **91**, 4801? (2010).

[31] J. D. Teufel, J. W. Harlow, C. A. Regal, and K. W. Lehnert, Phys. Rev. Lett. **101**, 197203 (2008).

[32] T. Rocheleau, T. Ndukum, C. Macklin, J. B. Hertzberg, A. A. Clerk, and K. C. Schwab, Nature **463**, 72 (2010).

[33] M. D. LaHaye, J. Suh, P. M. Echternach, K. C. Schwab, and M. L. Roukes, Nature **459**, 960 (2009).

[34] A. Voje, J. M. Kinaret, and A. Isacsson (2011), unpublished.

[35] R. J. Elliott, W. Hayes, G. D. Jones, H. F. MacDonald, and C. T. Sennett, Proc. R. Soc. Lond. A **289**, 1 (1965).

[36] M. Roukes, Phys. World **14**, 57 (2001).

[37] A. Eriksson, S. Lee, A. A. Sourab, A. Isacsson, R. Kaunisto, J. M. Kinaret, and E. E. B. Campbell, Nano Lett. **8**, 1224 (2008).

[38] Y. Xu, C. Chen, V. V. Deshpande, F. A. DiRenno, A. Gondarenko, D. B. Heinz, S. Liu, P. Kim, and J. Hone, Appl. Phys. Lett. **97**, 243111 (2010).

[39] R. G. Knobel and A. N. Cleland, Nature **424**, 291 (2003).

[40] R. Lifshitz and M. C. Cross, in *Reviews of Nonlinear Dynamics and Complexity* (Wiley-VCH, New York, 2008), vol. 1, [www.tau.ac.il/ ronlif/pubs/RNDC1-1-2008-preprint.pdf].

[41] M. I. Dykman and M. A. Krivoglaz, Phys. Stat. Sol. (b) **48**, 497 (1971).

[42] M. I. Dykman and M. A. Krivoglaz, Phys. Stat. Sol. (b) **68**, 111 (1975).

[43] S. Zaitsev, O. Shtempluck, E. Buks, and O. Gottlieb, arXiv:09110833v2 (2009).

[44] I. Kozinsky, H. W. C. Postma, I. Bargatin, and M. L. Roukes, Appl. Phys. Lett. **88**, 253101 (2006).

[45] J. S. Aldridge and A. N. Cleland, Phys. Rev. Lett. **94**, 156403 (2005).

[46] Q. P. Unterreithmeier, T. Faust, and J. P. Kotthaus, Phys. Rev. B **81**, 241405R (2010).

[47] D. Midtvedt, Y. Tarakanov, and J. M. Kinaret, Nano Lett. **11**, 1439 (2011).

[48] K. L. Turner, S. A. Miller, P. G. Hartwell, N. C. MacDonald, S. H. Strogatz, and S. G. Adams, Nature **396**, 149 (1998).

[49] S.-B. Shim, M. Imboden, and P. Mohanty, Science **316**, 95 (2007).

[50] I. Mahboob and H. Yamaguchi, Nature Nanotech. **3**, 275 (2008).

[51] J. Suh, M. D. LaHaye, P. M. Echternach, K. C. Schwab, and M. L. Roukes, Nano Lett. **10**, 3990 (2010).

[52] R. B. Karabalin, S. C. Masmanidis, and M. L. Roukes, Appl. Phys. Lett. **97**, 183101 (2010).

[53] I. Katz, A. Retzker, R. Straub, and R. Lifshitz, Phys. Rev. Lett. **99**, 040404 (2007).

[54] T. J. Kippenberg and K. J. Vahala, Science **321**, 1172 (2008).

[55] K. L. Ekinci, Y. T. Yang, and M. L. Roukes, J. Appl. Phys. **95**, 2682 (2004).

[56] A. N. Cleland and M. L. Roukes, J. Appl. Phys. **92**, 2758 (2002).

[57] H. J. Mamin and D. Rugar, Appl. Phys. Lett. **79**, 3358 (2001).

[58] J. D. Teufel, T. Donner, M. A. Castellanos-Beltran, J. W. Harlow, and K. W. Lehnert, Nature Nanotech. **4**, 820 (2009).

[59] I. Wilson-Rae, Phys. Rev. B **77**, 245418 (2008).

[60] M. Prunnila and J. Meltaus, Phys. Rev. Lett. **105**, 125501 (2010).

[61] E. M. Weig, R. H. Blick, T. Brandes, J. Kirschbaum, W. Wegscheider, M. Bichler, and J. P. Kotthaus, Phys. Rev. Lett. **92**, 046804 (2004).

[62] S. Sapmaz, P. Jarillo-Herrero, Y. M. Blanter, C. Dekker, and H. S. J. van der Zant, Phys. Rev. Lett. **96**, 026801 (2006).

[63] A. K. Hüttel, B. Witkamp, M. Leijnse, M. R. Wegewijs, and H. S. J. van der Zant, Phys. Rev. Lett. **102**, 225501 (2009).

[64] R. Leturcq, C. Stampfer, K. Inderbitzin, L. Durrer, C. Hierold, E. Mariani, M. G. Schultz, F. von Oppen, and K. Ensslin, Nat. Phys. **5**, 327 (2009).

[65] L. Y. Gorelik, A. Isacsson, M. V. Voinova, B. Kasemo, R. I. Shekhter, and M. Jonson, Phys. Rev. Lett. **80**, 4526 (1998).

[66] A. D. Armour, M. P. Blencowe, and Y. Zhang, Phys. Rev. B **69**, 125313 (2004).

[67] Y. M. Blanter, O. Usmani, and Y. V. Nazarov, Phys. Rev. Lett. **93**, 136802 (2004).

[68] F. Pistolesi and R. Fazio, Phys. Rev. Lett. **94**, 036806 (2005).

[69] D. Mozyrsky, M. B. Hastings, and I. Martin, Phys. Rev. B **73**, 035104 (2006).

[70] C. B. Doiron, W. Belzig, and C. Bruder, Phys. Rev. B **74**, 205336 (2006).

[71] O. Usmani, Y. M. Blanter, and Y. V. Nazarov, Phys. Rev. B **75**, 195312 (2007).

[72] F. Pistolesi and S. Labarthe, Phys. Rev. B **76**, 165317 (2007).

[73] F. Pistolesi, Y. M. Blanter, and I. Martin, Phys. Rev. B **78**, 085127 (2008).

[74] G. Weick, F. von Oppen, and F. Pistolesi, Phys. Rev. B **83**, 035420 (2011).

[75] A. A. Clerk and S. Bennett, New J. Phys. **7**, 238 (2005).

[76] A. Naik, O. Buu, M. D. LaHaye, A. D. Armour, A. A. Clerk, M. P. Blencowe, and K. C. Schwab, Nature **443**, 193 (2006).

[77] S. Zippilli, G. Morigi, and A. Bachtold, Phys. Rev. Lett. **102**, 096804 (2009).

[78] S.-H. Ouyang, J. Q. You, and F. Nori, Phys. Rev. B **79**, 075304 (2009).

[79] F. Santandrea, L. Y. Gorelik, R. I. Shekhter, and M. Jonson, Phys. Rev. Lett. **106**, 186803 (2011).

[80] G. Sonne and L. Y. Gorelik, Phys. Rev. Lett. **106**, 167205 (2011).

[81] M. T. Woodside and P. L. McEuen, Science **296**, 1098 (2002).

[82] J. Zhu, M. Brink, and P. L. McEuen, Appl. Phys. Lett. **87**, 242102 (2005).

[83] R. Stomp, Y. Miyahara, S. Schaer, Q. Sun, H. Guo, P. Grutter, S. Studenikin, P. Poole, and

A. Sachrajda, Phys. Rev. Lett. **94**, 056802 (2005).

[84] J. Zhu, M. Brink, and P. L. McEuen, Nano Lett. **8**, 2399 (2008).

[85] S. D. Bennett, L. Cockins, Y. Miyahara, P. Grutter, and A. A. Clerk, Phys. Rev. Lett. **104**, 017203 (2010).

[86] L. Cockins, Y. Miyahara, S. D. Bennett, A. A. Clerk, S. Studenikin, P. Poole, A. Sachrajda, and P. Grutter, Proc. Natl. Acad. Sci. USA **107**, 9496 (2010).